

Coherent perfect absorption in resonant materials

S. Shabahang, Ali. K. Jahromi, L. N. Pye, J. D. Perlstein, M. L. Villinger, and Ayman F. Abouraddy

CREOL, The College of Optics & Photonics, University of Central Florida, Orlando, Florida 32816, USA

E-mail: jahromi@creol.ucf.edu

September 2017

Abstract. Coherent perfect absorption (CPA) is an interferometric effect that guarantees full absorption in a lossy layer independently of its intrinsic losses. To date, it has been observed only at a single wavelength or narrow bandwidths, whereupon wavelength-dependent absorption can be ignored. Here we produce CPA over a bandwidth of ~ 60 nm in a $2\text{-}\mu\text{m}$ -thick polymer film with a low-doping concentration of an organic laser dye. A planar cavity is designed with a spectral ‘dip’ to accommodate the dye resonant linewidth, and CPA is thus achieved even at its absorption edges. This approach allows realizing strong absorption in laser dyes – and resonant materials in general – independently of the intrinsic absorption levels, with a flat spectral profile and without suffering absorption quenching due to high doping levels.

Keywords: optical cavity, interference, Fabry-Pérot resonator, resonant organic materials

Maximizing optical absorption is at the heart of enhancing the performance of a variety of photonic devices [1], such as photovoltaics [2, 3], photodetectors [4, 5], and laser gain media [6], and can even help introduce new functionalities [7, 8]. This goal can be realized via coherent perfect absorption (CPA) – an interferometric effect that guarantees complete absorption in a material independently of its intrinsic level [9, 10, 11, 12]. This powerful capability has prompted extensive efforts for realizing CPA in numerous settings including plasmonics and metasurfaces [11, 13, 14, 15, 16, 17], semiconductor [18, 19] and metal [20, 21] films, 2D materials [22, 23, 24], optical fibers [25], planar structures [26, 27, 28, 12, 29, 30], and on-chip systems [31, 32, 33]. However, all these realizations were made over narrow bandwidths or even at a single wavelength. *Broadband* CPA is a more demanding task because it must contend with wavelength-dependent absorption, which is most prominent in materials featuring resonant absorption, such as quantum dots, perovskites, and organic laser dyes – which are yet to be investigated in this context.

Here we realize CPA in weakly absorbing $2\text{-}\mu\text{m}$ -thick spin-coated polymer films impregnated with laser dyes: rhodamine 101 dye and DCM (4-(Dicyanomethylene)-2-

methyl-6-(4-dimethylaminostyryl)-4H-pyran) dye, which exhibit resonant absorption in the visible. This is achieved by embedding the doped polymer film in a planar cavity that incorporates aperiodic multilayer dielectric mirrors whose reflectivity is specially designed to inversely track the dispersive absorption of the dyes. By introducing an appropriate spectral ‘dip’ in the mirror reflectivity, spectrally flat coherently enhanced absorption is produced at cavity resonances spanning a bandwidth (~ 60 nm) larger than the dye linewidth. Rather than optimize the interference of counterpropagating beams within the absorbing structure [10, 26, 11], we critically couple a single beam to the cavity [30], which is a more appropriate configuration for applications in photovoltaics and photodetection. This strategy can help circumvent the challenge of concentration quenching in highly doped thin films by guaranteeing complete optical absorption independently of the doping level. Indeed, we observe an absorption enhancement by a factor of $\sim 12 - 25$ in the weakly absorbing, low-dye-concentration 2- μm -thick polymer films. Furthermore, we realized this effect in symmetric and asymmetric cavities, demonstrating the superiority of the latter when provided with a back-reflector. Finally, we show that adding a spacer to reduce the cavity free spectral range (FSR) does *not* impact the achievable absorption.

We first elucidate our strategy for achieving broadband CPA by considering a thin layer (thickness L) of a material (refractive index n) having a single-pass intensity absorption $\mathcal{A}(\lambda)$ placed in a planar cavity with front and back mirrors M_1 and M_2 of reflectivities R_1 and R_2 , respectively. A field incident normally on the cavity from the left produces transmitted T_L and reflected R_L waves, whereupon the total cavity absorption is \mathcal{A}_L ,

$$\mathcal{A}_L(\lambda) = 1 - T_L - R_L = \frac{(1 - R_1)(1 - \Gamma)(1 + \Gamma R_2)}{(1 - \Gamma\sqrt{R_1 R_2})^2 + 4\Gamma\sqrt{R_1 R_2} \sin^2 \frac{\varphi}{2}}; \quad (1)$$

where $\Gamma(\lambda) = 1 - \mathcal{A}(\lambda)$, $\varphi(\lambda) = 2\frac{2\pi}{\lambda}nL + \alpha_1 + \alpha_2$ is the round-trip phase, and α_1 and α_2 are

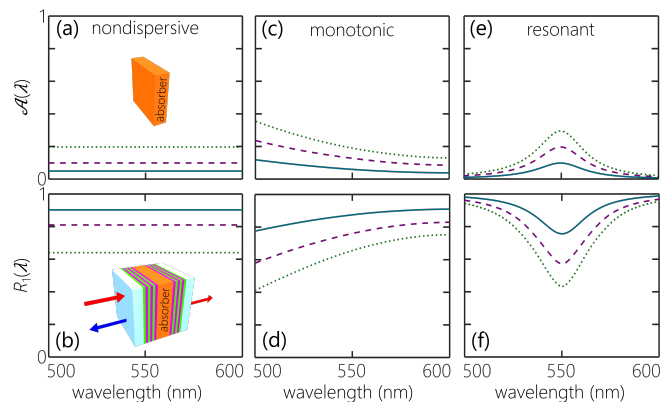


Figure 1: (a) Flat single-pass absorption $\mathcal{A}(\lambda)$ and (b) the reflectivity $R_1(\lambda) = (1 - \mathcal{A})^2$ required to achieve CPA ($\mathcal{A}_L = 1$) in the cavity shown in the inset. Dotted, dashed, and solid curves correspond to three different values for \mathcal{A} . (c,d) Same as (a,b) for a layer with monotonically decreasing $\mathcal{A}(\lambda)$. (e,f) Same as (a,b) for a layer with resonant absorption.

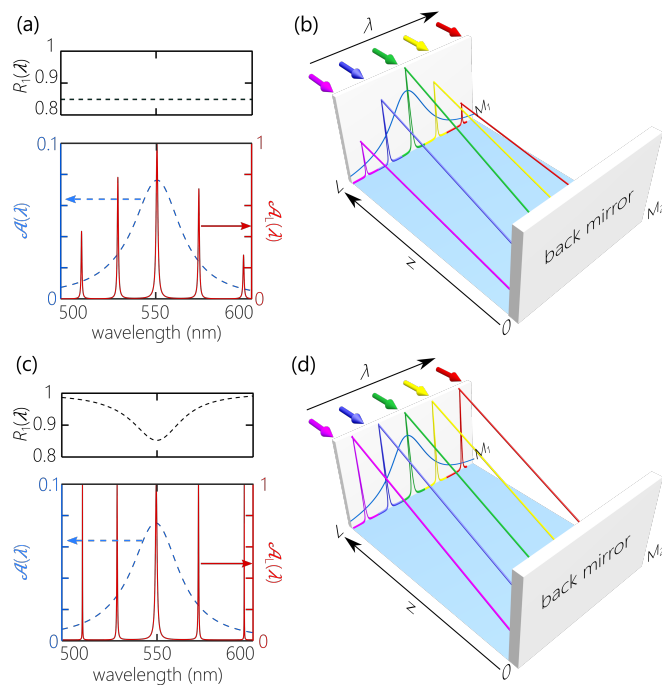


Figure 2: (a) Single-pass absorption $\mathcal{A}(\lambda)$ and total absorption $\mathcal{A}_L(\lambda)$ for a cavity whose front mirror has a flat spectral reflectivity $R_1(\lambda)$; CPA is achieved only at the central wavelength. (b) Axial decay of the normalized Poynting's vector along the cavity at the resonant wavelengths. Except for the central wavelength, the field is not critically coupled to the cavity, which results in only partial absorption. (c) Same as (a) for a CPA cavity whose front mirror has an appropriately designed reflectivity $R_1(\lambda)$. CPA is achieved across the whole spectrum. (d) Same as (b), except that the field is critically coupled at all the resonances.

the reflection phases from the M_1 and M_2 , respectively. Realizing full absorption $\mathcal{A}_L = 1$ implies that $T_L = R_L = 0$, which requires satisfying the following conditions: (i) $\varphi = m\pi$ for integer m , i.e., CPA occurs only at the cavity resonances; (ii) $R_2(\lambda) = 1$, which implies the need for a back-reflector; and (iii) $R_1(\lambda) = (1 - \mathcal{A}(\lambda))^2$, which necessitates utilizing a multilayer structure to produce a spectral reflectivity $R_1(\lambda)$ that tracks the material absorption. Three configurations are shown in Fig. 1. First, spectrally flat $\mathcal{A}(\lambda)$ (e.g., graphene) requires utilizing a mirror with constant $R_1(\lambda)$ [Fig. 1(a,b)]. Previous narrowband CPA observations fall into this class in which the wavelength-dependence of the intrinsic material absorption can be ignored. Second, monotonically *decreasing* $\mathcal{A}(\lambda)$ (e.g., Si in the near-infrared) requires monotonically *increasing* $R_1(\lambda)$ [Fig. 1(c,d)], as demonstrated in [30]. Third, resonant absorption (e.g., in an organic laser dye) requires a spectral *dip* in $R_1(\lambda)$ [Fig. 1(e,f)]. This latter configuration has *not* been realized to date to the best of our knowledge.

We consider a generic Lorentzian profile for the absorbing layer $\mathcal{A}(\omega) = \mathcal{A}_0 \frac{(\Delta\omega/2)^2}{(\omega - \omega_0)^2 + (\Delta\omega/2)^2}$, where ω_0 is the resonant frequency, $\Delta\omega$ is FWHM of the Lorentzian profile, and \mathcal{A}_0 is its peak absorption [Fig. 1(e)]. Placing such a layer in a planar cavity with a back-reflector $R_2(\lambda) = 1$ and a front mirror with flat spectral reflectivity R_1 can help realize CPA at one resonance (e.g., at $\lambda = \lambda_0$ if $R_1 = (1 - \mathcal{A}_0)^2$), but

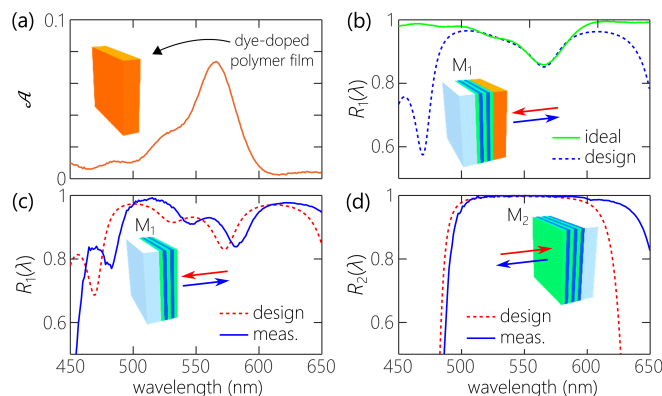


Figure 3: (a) Measured single-pass absorption $\mathcal{A}(\lambda)$ for a 2- μm -thick PMMA layer doped with rhodamine 101. (b) The ideal reflectivity $R_1(\lambda) = (1 - \mathcal{A})^2$ to realize CPA for the layer in (a) and the approximate design over the bandwidth of interest 500-600 nm (assuming incidence from PMMA). (c) The designed and measured front mirror reflectivity $R_1(\lambda)$ for incidence from free-space. (d) The designed and measured back mirror reflection $R_2(\lambda)$.

the absorption drops at all the others resonances [Fig. 2(a)] because their coupling coefficients to the cavity (normalized with respect to the incident vales) are less than unity [Fig. 2(b)]. Poynting's vector along the cavity in presence of the back-reflector is $P(z) = \mathcal{A}_L(\lambda) \frac{\sinh[\alpha(\lambda)z]}{\sinh[\alpha(\lambda)L]}$, where $\alpha(\lambda)$ is the absorption coefficient, $\Gamma(\lambda) = e^{-\alpha(\lambda)L}$, and z is measured from M_2 [Fig. 2(b)]. In contrast, if the front mirror reflectivity is $R_1(\lambda) = (1 - \mathcal{A}(\lambda))^2$, which thus has an appropriately shaped dip at $\lambda = \lambda_0 = 2\pi c/\omega_0$ (c is speed of light in vacuum), then *all* the resonances exhibit complete absorption $\mathcal{A}_L = 1$ across the whole spectrum independently of $\mathcal{A}(\lambda)$ [Fig. 2(c)]. In this case, the field coupling to the cavity is unity at all wavelengths, and the normalized Poynting's vector decays according to $P(z) = \frac{\sinh[\alpha(\lambda)z]}{\sinh[\alpha(\lambda)L]}$ [Fig. 2(d)]. In a weakly absorbing layer $\alpha(\lambda) \ll \frac{1}{L}$, Poynting's vector decays linearly along the cavity, $P(z) \approx \frac{z}{L}$, independently of $\alpha(\lambda)$ and thus also of λ . Moreover, perfect resonant absorption is possible even if the intrinsic absorption $\mathcal{A}(\lambda)$ does *not* conform to a Lorentzian profile, as long as $R_1(\lambda)$ is judiciously engineered.

Guided by this model, we realize CPA over a broad bandwidth (~ 60 nm) in a weakly absorbing 2- μm -thick PMMA film doped with rhodamine 110, having a single-pass absorption peak of $\mathcal{A}_0 \approx 7.5\%$ [Fig. 3(a)]. We designed a multilayer front mirror M_1 (using the software package FilmStar) whose reflectivity approximates the ideal target of $R_1(\lambda) = (1 - \mathcal{A}(\lambda))^2$ over the spectral range 500 – 600 nm, and comprises 21 bilayers of SiO_2 (refractive index is $n \approx 1.5$) and TiO_2 ($n \approx 2.4$) [Fig. 3(b)]. We fabricated this front mirror by physical vapor deposition, and the measured reflection spectrum is shown in Fig. 3(c). The formula $R_1(\lambda) = (1 - \mathcal{A}(\lambda))^2$ refers to the reflectivity of a field incident from the absorbing layer and *not* from free space [12]. The calculated spectrum in Fig. 3(c) takes into consideration the necessary modification in $R_1(\lambda)$ [30]. The measurement reveals an excellent match with theory except for a ≈ 10 nm spectral red-shift with respect to the ideal spectrum. The back-reflector M_2 is a periodic Bragg

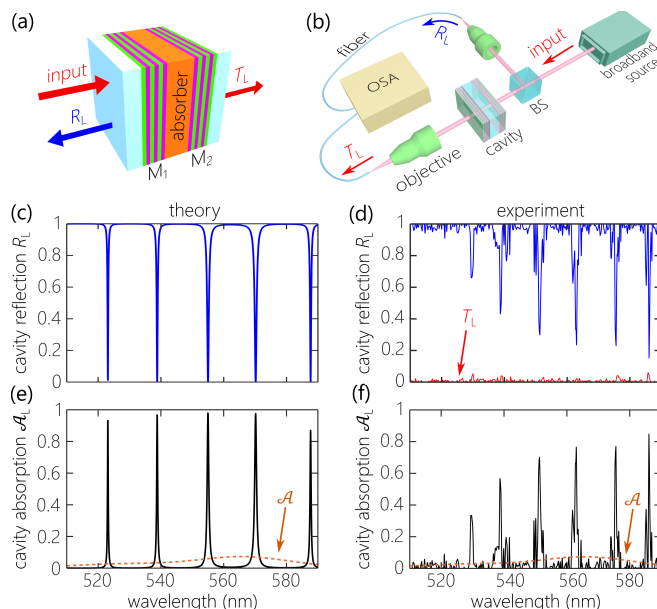


Figure 4: (a) CPA cavity structure. (b) schematic of the setup for to measure $\mathcal{A}_L(\lambda)$. The transmitted and reflected fields are collected and coupled via fibers to an optical spectrum analyzer (OSA). (c) The calculated and (d) measured cavity reflection $R_L(\lambda)$; the transmission $T_L(\lambda)$ is negligible because $R_2 \approx 1$. (e) The calculated and (f) measured the cavity absorption $\mathcal{A}_L(\lambda) = 1 - T_L(\lambda) - R_L(\lambda)$. A large enhancement in the resonant absorption is clear compared to the single-pass absorption $\mathcal{A}(\lambda)$.

reflector comprising 21 alternating quarter-wavelength layers of SiO_2 and TiO_2 , which yields a near-unity flat spectral reflectivity $R_2(\lambda) \approx 1$ [Fig. 3(d)].

Using the mirrors M_1 and M_2 whose reflectivities satisfy the desiderata for CPA, we construct an asymmetric planar cavity by spin-coating a PMMA-dye solution on the back mirror and then sandwiching the polymer layer between the mirrors [Fig. 4(a)]. We measured the cavity absorption $\mathcal{A}_L(\lambda)$ utilizing the setup depicted schematically in Fig. 4(b). A collimated beam from a broadband incoherent light source (a Tungsten lamp) is directed to the cavity and the transmitted T_L and reflected R_L beams are collected and delivered via multimode fibers (50- μm core diameter) to an optical spectrum analyzer (OSA), from which we obtain the total absorption $\mathcal{A}_L = 1 - T_L - R_L$. We plot in Fig. 4(c,d) the calculated and measured spectral reflectivity $R_L(\lambda)$; the measured spectral transmission $T_L(\lambda)$ is negligible as expected. The calculated and measured spectral absorption in the cavity $\mathcal{A}_L(\lambda)$ are plotted in Fig. 4(e,f), along with the measured single-pass absorption $\mathcal{A}(\lambda)$ from Fig. 3(a).

We can draw several conclusions from the results in Fig. 4. First, the structure produces an absorption enhancement $\mathcal{A}_L(\lambda)/\mathcal{A}_0 \approx 12 - 25$ at the cavity resonances. Second, this absorption enhancement is produced over a broad bandwidth ~ 60 nm, which extends to the edges of the dye absorption linewidth. Even resonances that are strongly displaced from the rhodamine absorption-peak wavelength exhibit significantly higher absorption $\mathcal{A}_L(\lambda)$ than the single-pass absorption $\mathcal{A}(\lambda)$ at the same wavelength.

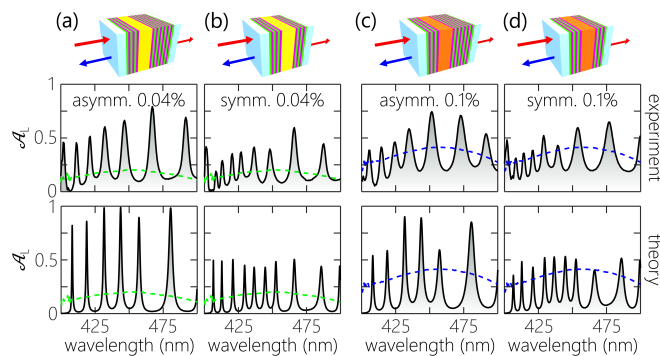


Figure 5: (a) Absorption spectrum for two $\approx 2\text{-}\mu\text{m}$ -thick films of DCM-doped PMMA at different concentration levels. (b) The symmetric (right column) and asymmetric (left column) cavity for a DCM concentration of 0.04%. The cavities are illuminated from left, and the measured absorption is compared with theoretical expectations (bottom row). The results indicate the enhanced resonant absorption can reach close to 100% in the asymmetric device, while it cannot increase much further beyond 50% for the symmetric cavity. (c) Same as (b), with 0.1% DCM concentration. The dashed curves throughout are the single-pass absorption $\mathcal{A}(\lambda)$.

The mirror design guarantees a perfect resonant absorption across the whole bandwidth, independently of the intrinsic spectral absorption of the organic film. The decay in the absorption enhancement at the edges of this spectral range is likely due to the deviation in $R_1(\lambda)$ of the fabricated front mirror with respect to the targeted design [Fig. 3(c)].

To further confirm this effect, we implemented the same procedure with DCM. We tested two single-pass absorption levels \mathcal{A} produced by varying the DCM concentration in a $\approx 2\text{-}\mu\text{m}$ -thick PMMA layer [Fig. 5]. Furthermore, we studied the absorption in two different cavity structures: (1) an *asymmetric* structure similar to that utilized above with $R_1(\lambda) = (1 - \mathcal{A}(\lambda))^2$ and $R_2(\lambda) = 1$, whereupon CPA ($\mathcal{A}_L = 1$) can be ideally achieved; and (2) a *symmetric* cavity in which $R_1(\lambda) = R_2(\lambda)$. In the latter case, the cavity achieves an *optimal* absorption of $\mathcal{A}_L = \frac{1}{8} \frac{(2-\mathcal{A})^2}{1-\mathcal{A}}$ when $R_1(\lambda) = R_2(\lambda) = 1 - \mathcal{A}(\lambda)$ [12]. Here CPA cannot be achieved. Instead, an optimal absorption of *at least* $\mathcal{A}_L = \frac{1}{2}$ is guaranteed even for vanishingly small \mathcal{A} , and a maximum optimal absorption of $\mathcal{A}_L = \frac{2}{3}$ is reached when $\mathcal{A} = \frac{2}{3}$ (for $\mathcal{A} > \frac{2}{3}$, the optical absorption is $\mathcal{A}_L = \mathcal{A}$) [12].

Calculated and measured absorption spectra are plotted in Fig. 5(a,b) for the asymmetric and symmetric cavities for a DCM concentration of 0.04%, and for a DCM concentration of 0.1% in Fig. 5(c,d). The mirrors in all four cavities are constructed of alternating layers of Nb_2O_5 ($n \approx 2.25$) and SiO_2 , optimized using the same approach outlined above. The results confirm both the broadband absorption enhancement in the cavity above that of the single-pass absorption, and also confirms that the absorption peaks for the symmetric cavities only slightly exceed 50%. Note that the absorption enhancement is larger for the case of lower dye concentration.

Finally, we carried out an experiment to ensure that increasing the cavity size (thus reducing its FSR) by inserting a passive spacer within the cavity does not reduce

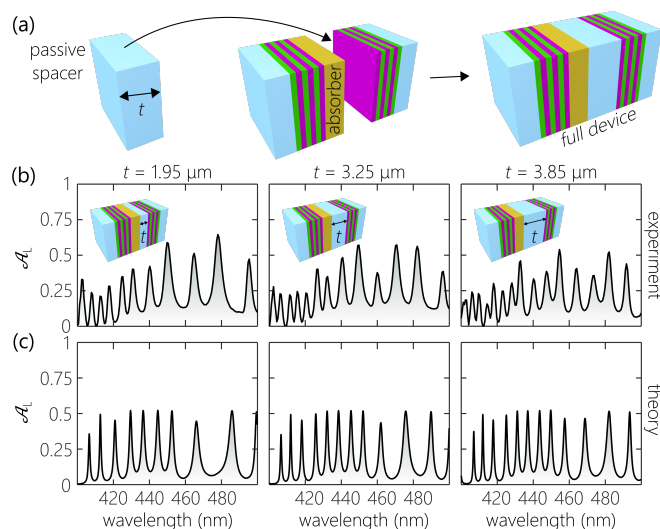


Figure 6: (a) Construction of a symmetric planar cavity containing a $\approx 2\text{-}\mu\text{m}$ -thick polymer film doped with 0.1% DCM dye [Fig. 5(c,d)] and also incorporates a transparent silica spacer. Three such devices are produced with different spacer thickness t adjacent to the absorbing film. (b) The measured and (c) the calculated absorption spectra for spacer thicknesses of $t = 1.95\mu\text{m}$ (left column), $t = 3.25\mu\text{m}$ (middle column) and $t = 3.85\mu\text{m}$ (right column). The results indicate no significant impact of the extra spacer thickness on the resonantly enhanced absorption, while it increases the number of resonances (reduces the FSR) because of the increased cavity length.

the resonant enhancement in absorption, and can indeed be useful in engineering the absorption spectrum. Using the 0.1%-concentration DCM layer from Fig. 5(c,d), we construct three symmetric cavities using the same mirror reflectivities, but with different-thickness silica spacers deposited on M_2 [Fig. 6(a)]. The calculated and measured absorption spectra $\mathcal{A}_L(\lambda)$ plotted in Fig. 6(b,c) confirm that a passive spacer does *not* have a detrimental impact on the absorption except for increasing the number of resonances and reducing the FSR.

Our strategy to realize CPA is materials-agnostic, and is thus applicable to other material systems with different underlying absorption mechanisms. The measurements confirm CPA at the discrete wavelengths associated with the cavity structure. We have recently shown that these resonances can be broadened to extend over extended spectral ranges *without* modifying the cavity itself via a strategy that we have called ‘omni-resonance’ [34, 35, 36]. Applying this approach here would yield broadband, continuous wavelength CPA in resonant optical materials. Finally, the approach outlined here when combined with omni-resonance can also benefit pump gain media [37] and even contribute to reduced-threshold lasing [38] and non-Hermitian optics in general.

In conclusion, we have proposed a generic design for achieving CPA in resonant materials such as organic laser dyes, and experimentally demonstrated the concept with rhodamine 101 and DCM dyes. An appropriate planar photonic environment containing a mirror featuring a spectral reflectivity dip guarantees that a weakly absorbing layer

absorbs light fully, independently of its intrinsic absorption level – realized with a flat absorption spectrum. Our materials-agnostic approach is independent of the spectral range or target bandwidth. This strategy that combines the simplicity of a planar structure with the convenience of a non-interferometric configuration (only a single incident beam) can be useful in a variety of applications, including photodetectors, solar cells, and optical switches.

Funding

Air Force Office of Scientific Research (AFOSR) under MURI award FA9550-14-1-0037.

Acknowledgments

The authors are grateful to Nathan Bodnar for technical assistance.

References

- [1] D. G. Baranov, A. Krasnok, T. Shegai, A. Alú, and Y. Chong. Coherent perfect absorbers: linear control of light with light. *Nat. Rev. Mater.*, 2:17064, 2017.
- [2] Zongfu Yu, Aaswath Raman, and Shanhui Fan. Fundamental limit of nanophotonic light trapping in solar cells. *Proc. Natl Acad. Sci. USA*, 107:17491–17496, 2010.
- [3] M. L. Villinger, A. Shiri, S. Shabahang, A. K. Jahromi, M. B. Nasr, C. Villinger, and A. F. Abouraddy. Doubling the near-infrared photocurrent in a solar cell via omni-resonant coherent perfect absorption. *arXiv:1911.09276*, 2019.
- [4] J. Muller. Thin silicon film p-i-n photodiodes with internal reflection. *IEEE Trans. Electron Devices*, 25:247 – 253, 1978.
- [5] M. S. Ünlü and S. Strite. Resonant cavity enhanced photonic devices. *J. Appl. Phys.*, 78:607–639, 1995.
- [6] W.J. Kozlovsky and W.P. Risk. Efficient diode-laser-pumped 946 nm Nd:YAG laser with resonator-enhanced pump absorption. *IEEE J. Quantum Electron.*, 28:1139–1141, 1992.
- [7] X. Fang, K. F. MacDonald, and N. I. Zheludev. Controlling light with light using coherent metadevices: all-optical transistor, summator and inverter. *Light Sci. Appl.*, 4:e292, 2015.
- [8] M. Papaioannou, E. Plum, J. Valente, E. T. F. Rogers, and N. I. Zheludev. All-optical multichannel logic based on coherent perfect absorption in a plasmonic metamaterial. *APL Photonics*, 1:090801, 2016.
- [9] Y. D. Chong, L. Ge, H. Cao, and A. D. Stone. Coherent perfect absorbers: Time-reversed lasers. *Phys. Rev. Lett.*, 105:053901, 2010.
- [10] W. Wan, Y. Chong, L. Ge, H. Noh, A. D. Stone, and H. Cao. Time-reversed lasing and interferometric control of absorption. *Science*, 331:889–892, 2011.
- [11] J. Zhang, K. F. MacDonald, and N. I. Zheludev. Controlling light-with-light without nonlinearity. *Light Sci. Appl.*, 1:e18, 2012.
- [12] M. L. Villinger, M. Bayat, L. N. Pye, and A. F. Abouraddy. Analytical model for coherent perfect absorption in one-dimensional photonic structures. *Opt. Lett.*, 40:5550–5553, 2015.
- [13] J. W. Yoon, G. M. Koh, S. H. Song, and R. Magnusson. Measurement and modeling of a complete optical absorption and scattering by coherent surface plasmon-polariton excitation using a silver thin-film grating. *Phys. Rev. Lett.*, 109:257402, 2012.
- [14] M. S. Jang, V. W. Brar, M. C. Sherrott, J. J. Lopez, L. Kim, S. Kim, M. Choi, and H. A. Atwater.

- Tunable large resonant absorption in a midinfrared graphene salisbury screen. *Phys. Rev. B*, 90:165409, 2014.
- [15] T. Roger, S. Vezzoli, E. Bolduc, J. Valente, J. J. F. Heitz, J. Jeffers, C. Soci, J. Leach, C. Couteau, N. I. Zheludev, and D. Faccio. Coherent perfect absorption in deeply subwavelength films in the single-photon regime. *Nat. Commun.*, 6:7031, 2015.
- [16] M. J. Jung, C. Han, J. W. Yoon, and S. H. Song. Temperature and gain tuning of plasmonic coherent perfect absorbers. *Opt. Express*, 23:19837–19845, 2015.
- [17] G. Pirruccio, M. Ramezani, S. R.-K. Rodriguez, and J. G. Rivas. Coherent control of the optical absorption in a plasmonic lattice coupled to a luminescent layer. *Phys. Rev. Lett.*, 116:103002, 2016.
- [18] G. Ramakrishnan, G. K. P. Ramanandan, A. J. L. Adam, M. Xu, N. Kumar, R. W. A. Hendrikx, and P. C. M. Planken. Enhanced terahertz emission by coherent optical absorption in ultrathin semiconductor films on metals. *Opt. Express*, 21:16784–16798, 2013.
- [19] K. Xua, L. Huangb, Z. Zhangb, J. Zhaoa, Z. Zhangb, L. W. Snymanc, and J. W. Swart. Light emission from a poly-silicon device with carrier injection engineering. *Mater. Sci. Eng. B*, 231:28–31, 2018.
- [20] H. Pohlack and E. Hacker. Induced resonance absorption (indab) in thin films – a current example for versatile and efficient use of optical coating in semi-optical processes. *Proc. SPIE*, 1782:122–132, 1992.
- [21] P. Heger, O. Stenzel, and N. Kaiser. Metal island films for optics. *Proc. SPIE*, 5250:21–28, 2004.
- [22] G. Pirruccio, L. M. Moreno, G. Lozano, and J. G. Rivas. Coherent and broadband enhanced optical absorption in graphene. *ACS Nano*, 7:4810–4817, 2013.
- [23] S. M. Rao, J. J. F. Heitz, T. Roger, N. Westerberg, and D. Faccio. Coherent control of light interaction with graphene. *Opt. Lett.*, 39:5345–5347, 2014.
- [24] L. Huang, G. Li, A. Gurarslan, Y. Yu, R. Kirste, W. Guo, J. Zhao, R. Collazo, Z. Sitar, G. N. Parsons, M. Kudenov, and L. Cao. Atomically thin MoS₂ narrowband and broadband light superabsorbers. *ACS Nano*, 10:7493–7499, 2016.
- [25] A. K. Jahromi, A. Van Newkirk, and A. F. Abouraddy. Coherent perfect absorption in a weakly absorbing fiber. *IEEE Photonics J.*, 10:6500810, 2018.
- [26] C. Schmidt, M. Sudzius, S. Meister, H. Fröb, and K. Leo. Controllable coherent absorption of counterpropagating laser beams in organic microcavities. *Appl. Phys. Lett.*, 117:053301, 2020.
- [27] M. A. Kats, D. Sharma, J. Lin, P. Genevet, R. Blanchard, Z. Yang, M. M. Qazilbash, D. N. Basov, S. Ramanathan, and F. Capasso. Ultra-thin perfect absorber employing a tunable phase change material. *Appl. Phys. Lett.*, 101:221101, 2012.
- [28] M. Furchi, A. Urich, A. Pospischil, G. Lilley, K. Unterrainer, H. Detz, P. Klang, A. M. Andrews, W. Schrenk, G. Strasser, and T. Mueller. Tunable large resonant absorption in a midinfrared graphene salisbury screen. *Phys. Rev. B*, 90:165409, 2014.
- [29] N. Kakenov, O. Balci, T. Takan, V. A. Ozkan, H. Altan, and C. Kocabas. Observation of gate-tunable coherent perfect absorption of terahertz radiation in graphene. *PACS Photonics*, 3:1531–1535, 2016.
- [30] Lorelle N. Pye, Massimo L. Villinger, Soroush Shabahang, Walker D. Larson, Lane Martin, and Ayman F. Abouraddy. Octave-spanning coherent perfect absorption in a thin silicon film. *Opt. Lett.*, 42:151–154, 2017.
- [31] J. M. Rothenberg, C. P. Chen, J. J. Ackert, J. I. Dadap, A. P. Knights, K. Bergman, R. M. Osgood Jr., and R. R. Grote. Experimental demonstration of coherent perfect absorption in a silicon photonic racetrack resonator. *Opt. Lett.*, 41:2537–2540, 2016.
- [32] H. Zhao, W. S. Fegadolli, J. Yu, Z. Zhang, L. Ge, A. Scherer, and L. Feng. Metawaveguide for asymmetric interferometric light-light switching. *Phys. Rev. Lett.*, 117:193901, 2016.
- [33] Z. J. Wong, Y.-L. Xu, J. Kim, K. O’Brien, Y. Wang, L. Feng, and X. Zhang. Lasing and anti-lasing in a single cavity. *Nat. Photonics*, 10:796–801, 2016.
- [34] S. Shabahang, H. E. Kondakci, M. L. Villinger, J. D. Perlstein, A. El Halawany, and A. F.

- Abouraddy. Omni-resonant optical micro-cavity. *Sci. Rep.*, 7:10336, 2017.
- [35] S. Shabahang, A. K. Jahromi, A. Shiri, K. L. Schepler, and A. F. Abouraddy. Toggling between active and passive imaging with an omni-resonant micro-cavity. *Opt. Lett.*, 44:1532–1535, 2019.
- [36] A. Shiri, M. Yessenov, R. Aravindakshan, and A. F. Abouraddy. Omni-resonant space-time wave packets. *Opt. Lett.*, 45:1774–1777, 2020.
- [37] A. K. Jahromi, S. Shabahang, H. E. Kondakci, P. Melanen, S. Orsila, and A. F. Abouraddy. Transparent perfect mirror. *ACS Photonics*, 4:1026–1032, 2017.
- [38] A. K. Jahromi, A. U. Hassan, D. N. Christodoulides, and A. F. Abouraddy. Statistical parity-time-symmetric lasing in an optical fibre network. *Nat. Commun.*, 8:1359, 2017.